# DISPENSER PRINTING FOR PROTOTYPING MICROSCALE DEVICES

**Paul K. Wright, David A. Dornfeld, and Alic Chen**
**Department of Mechanical Engineering**
**and**
**Christine C. Ho and James W. Evans**
**Department of Materials Science and Engineering**
**University of California-Berkeley**
**Berkeley, CA**

**KEYWORDS**

Direct writing, Dispenser printing, Microscale devices, Prototyping

**ABSTRACT**

Direct write dispenser printing technology is a versatile and scalable manufacturing technique for additive deposition of novel materials. We present a versatile prototyping dispenser printer capable of rapid fabrication of unique microscale devices. A theoretical error analysis of the printer is performed to evaluate the repeatability and accuracy of the system. Additionally, we demonstrate two microdevice applications manufactured using the dispenser printer, including an electrochemical energy storage device and a thermoelectric energy harvester.

## INTRODUCTION

Recent advances in manufacturing technologies have led to the emergence of digital printing or direct writing as a scalable fabrication technique for electronics (Lewis et al., 2004). Direct write technology includes a range of versatile and scalable processes for the deposition of functional materials to form simple linear or complex conformal structures on a substrate. This technology can be integrated into existing manufacturing techniques for high-throughput volume production, particularly in microelectronics. Direct write processes of varying actuation, including inkjet, laser, flow, and tip printing have been used to produce feature sizes in the nanometer to millimeter range (Hon et al., 2008). “Inks” such as suspensions, slurries, and solutions of a variety of materials, including metals, ceramics, polymers, and biomaterials can be printed.

Dispenser tip printing is a type of flow-based direct writing technology that allows for on-demand patterning of materials at room temperature and ambient conditions. As a consequence, negligible materials waste is generated, and minimal energy expenditure is required for the operation of this process, leaving a small environmental footprint. Ink is extruded from a syringe needle directly onto a substrate in an additive fashion by pneumatic control. A large range of materials can be dispenser printed onto a variety of substrates including printed circuit boards (PCB), glass slides and silicon wafers. This method can be used for mass manufacturing by using multiple dispenser heads in an assembly line.

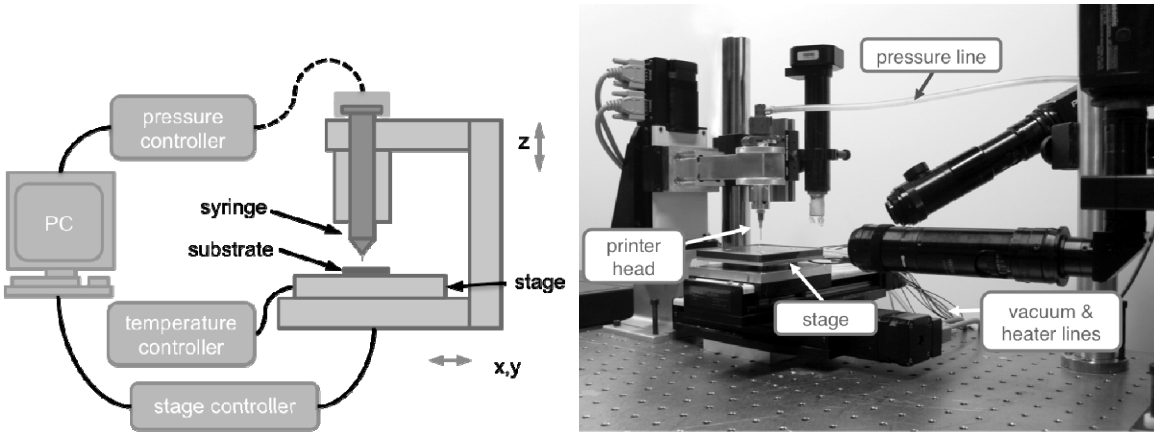


FIGURE 1. SCHEMATIC AND IMAGE OF PROTOTYPING DISPENSER PRINTER.

While direct write printing technologies are scalable towards mass manufacturing, prototyping-scale instruments are essential for on-demand deposition of unique materials and rapid design of interesting patterns, architectures, and devices. Thus, we have developed a prototyping dispenser printer for research of novel printed materials and microscale devices.

## DISPENSER PRINTING

The prototyping dispenser printer presented in this work consists of a three-axis stage, a pneumatically controlled dispensing syringe head, and a heated vacuum chuck stage. Figure 1 shows an image and schematic of the dispenser printer. The printer stages are Newmark Systems NLS4 series stages with 0.03 µm resolution and 5 µm repeatability (based on manufacturer's specifications). The stage controller is a Newmark Systems MSC-M four-axis stage controller and has 1 µm resolution (based on the manufacturer's specifications). Side-view and angled-view cameras are used to image the printer tip relative to the substrate. A top-down camera is used for custom-developed automated software alignment of the dispensing tip. The printer allows for deposition of inks of a wide range of viscosities from 100-10,000 cP, and is controlled using a Musashi ML-808FX pneumatic controller capable of 20–500 kPa output. All equipment is interfaced and controlled through a personal computer running custom Java software. Feature sizes down to 50 µm can be printed with film thicknesses ranging from 10 to 200 µm per pass, depending on a combination of process parameters such as shot pressure, tip size, rheology of the ink, and shot spacing. These parameters are all easily tuned within the automated software and allow for rapid adjustments to the process parameters in real time. Ink viscosity can be tuned by adjusting the amount of solvent/diluent in the mixture (which is removed upon drying), while tip sizes are adjusted by using commercially available disposable plastic and metal syringe tips. These tips are available in sizes ranging from several mm down to 100 µm in inner diameter, and smaller tips under 100 µm in inner diameter can be manually pulled from borosilicate glass pipettes. Kapton heaters are also bonded to the stage to allow heating up to 100°C for on-contact drying.

### Manufacturing Precision of Dispenser Printer

Printing of microscale devices requires high accuracy and repeatability, and thus these parameters must be assessed to understand possible errors during device fabrication. Figure 2 represents the structural loop of the dispenser micro-printer. The printing system is mounted to a vibration-isolated optical table (Newport LW2048B-OPT), which is used as the reference point in the structural loop. Stages X (1) and Y (2) can move independent of each other and are computer controlled to position the substrate (3).

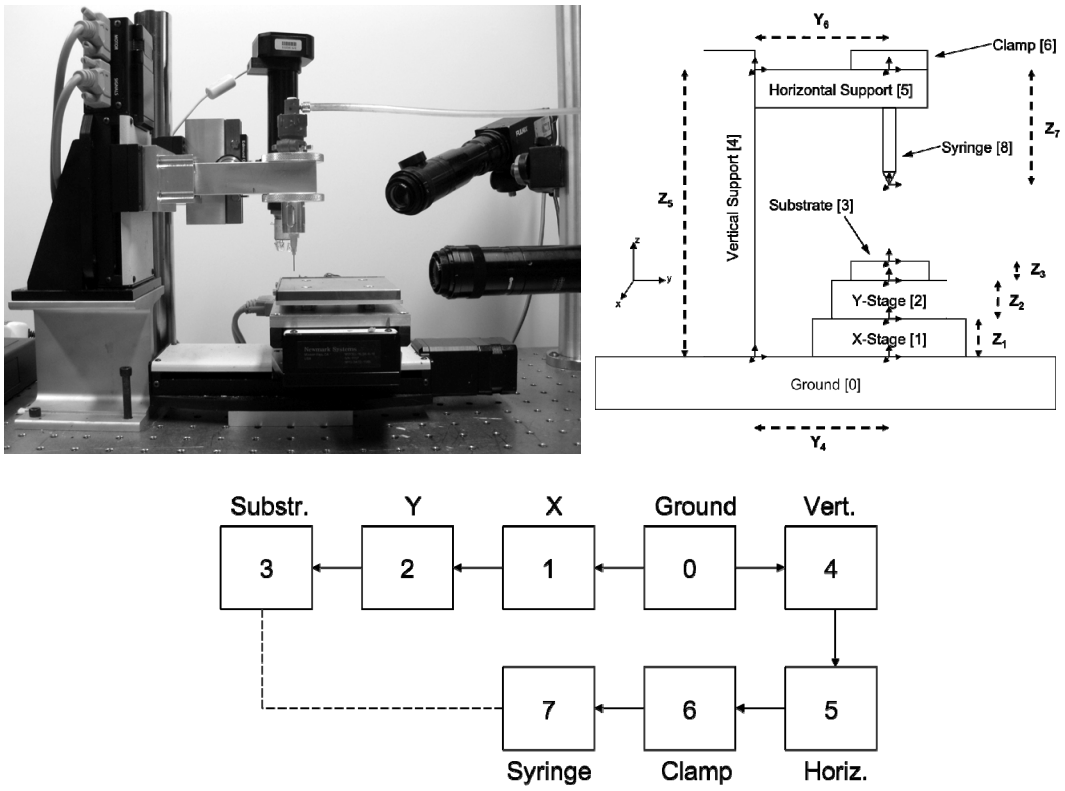


FIGURE 2. SCHEMATIC AND STRUCTURAL LOOP OF DISPENSER PRINTER.

Adjustments in (1) and (2) must be initiated to remove any positioning offsets between the substrate and the stage.

The overall objective is to obtain information about the relative position of the syringe (7) to the substrate (3). The structural loop is used to identify the errors in the path to the syringe. A vertical support column (4) is bolted onto the vibration-isolated table. A horizontal support (5) is then clamped onto the vertical support column. A custom-built aluminum clamp (6) is used to attach the syringe (7) onto the horizontal support (5).

To examine the errors of the system, a Homogenous Transform Matrix (HTM) analysis is performed to formulate an error matrix for the printer and determine the primary sources of error in the system:

| | $\delta_{x,T}$ | $\delta_{y,T}$ | $\delta_{z,T}$ |
|---|---|---|---|
| $\delta_{y,1}$ | $0$ | $1$ | $0$ |
| $\delta_{x,2}$ | $1$ | $0$ | $0$ |
| $\delta_{x,3}$ | $1$ | $0$ | $0$ |
| $\delta_{y,3}$ | $0$ | $1$ | $0$ |
| $\varepsilon_{z,3}$ | $Y_6 + \delta_{y,7} + \frac{Y_4}{1+(\varepsilon_{z,5})^2}$ | $-\delta_{y,7} - \frac{Y_4\varepsilon_{z,5}}{1+(\varepsilon_{z,5})^2}$ | $0$ |
| $\varepsilon_{z,5}$ | $-\frac{Y_4}{1+(\varepsilon_{z,5})^2}$ | $-\frac{Y_4\varepsilon_{z,5}}{1+(\varepsilon_{z,5})^2}$ | $0$ |
| $\delta_{z,5}$ | $0$ | $0$ | $-1$ |
| $\delta_{z,6}$ | $0$ | $0$ | $-1$ |
| $\delta_{x,7}$ | $-1$ | $-\varepsilon_{z,3}$ | $0$ |
| $\delta_{y,7}$ | $\varepsilon_{z,3}$ | $1$ | $0$ |

where the sources of each error term are defined as follows:

- $\delta_{y,1}$, $\delta_{x,2}$, $\delta_{z,5}$ are the inherent repeatability errors in the linear stages
- $\varepsilon_{z,5}$ is the Z support column rotational misalignment
- $\delta_{x,3}$ and $\delta_{y,3}$ are the offsets between the coordinate systems of the printer and the substrate
- $\varepsilon_{z,.3}$ is substrate rotation misalignment
- $\delta_{x,7}$, $\delta_{y,7}$ represent the effective play at the end of the syringe while clamped in the print head

$\varepsilon_{z,5}$ is minimal and can be eliminated by proper setup of the machine, similar to setting the tram of a milling machine. $\varepsilon_{z,3}$, $\delta_{x,3}$, and $\delta_{y,3}$ are arbitrary in the current usage of the machine, as the substrate is placed anywhere in the working space on the printer stage, and can be the main sources of misalignment in the current use of the printer**.** These errors are currently resolved by using flat-edge right-angled substrates aligned along the corner of the substrate stage. $\delta_{x,7}$ and $\delta_{y,7}$ terms are compensated by using a short horizontal support with a base plate and fitted syringe holder to dampen the play of the syringe tip from the pressure in the air line. The results of the HTM analysis provide a baseline understanding of possible errors in device manufacturing, but the repeatability and error of the dispenser printer can be further analyzed. Additionally, a programmable alignment system for automated dispensing of high-density arrays is currently being investigated. The alignment system will also work to solve error offsets, $\varepsilon_{z,3}$, $\delta_{x,3}$, and $\delta_{y,3}$, from substrate placement.

## PRINTABLE MICROSCALE APPLICATIONS

The dispenser printer is a versatile fabrication tool capable of bridging the technology disparity between microfabrication processes (capable of patterning micron-scale features and smaller) and larger-scale processes (such as screen-printing and bulk processes able to pattern feature sizes ranging from tens to hundreds of microns). It has the unique ability to pattern lateral and vertical dimensions within 10–200 µm feature sizes and with dispenser printing intricate two-dimensional patterns, as well as three-dimensional structures, have been fabricated. In the next sections we highlight two microscale devices with different architectures, both of which exhibited optimal performances when patterned using dispenser printing. With these prototyping examples, we demonstrate the diverse capabilities of the dispenser printer system.

### Electrochemical Energy Storage Devices

The integration of micropower supplies for microdevices has proven to be an exacting challenge. Crowded substrates have limited unused area and little footprint area is available for depositing a battery or electrochemical capacitor component. These devices are multi-layer sandwich structures with two electrodes sandwiching an electrolyte layer. The electrodes provide the interfaces at which energy storage occurs, either by chemical energy conversion in batteries or electrostatic phenomena in electrochemical capacitors. As a result, the storage capacity scales with the amount of electrode materials deposited for small footprint energy storage devices (<1 $cm^2$). Some of the most advanced microbatteries available today are deposited using thin-film vapor-phase deposition techniques such as sputtering or pulsed laser deposition, and are capable of depositing films with maximum thicknesses in the sub-micron range. Due to difficulties with stresses accumulating in the vapor deposited films, as well as adhesion issues, deposition of thicker films is not feasible. As a consequence, microbatteries and microcapacitors fabricated using thin film techniques are often limited to capacities of 0.1 mAh/$cm^2$ (Dudney, 2005), and capacitances of 30 mF/$cm^2$, respectively (Lim et al., 2001).

Order of magnitude improvements in the performance values of both electrochemical devices can be achieved through the use of thick-film deposition technology such as dispenser printing. As illustrated in Figures 3 and 4, stacked, multilayer battery and capacitor structures have been fabricated using the dispenser printer and electrode thicknesses of 30–70 µm have been deposited. The layer thicknesses can be tailored specifically for an application's demands. Flat, conformal films are printed in successive layer-by-layer fashion, with short drying steps of 70°C between each deposition and good adhesion is attained at each interface. Zinc-metal oxide batteries with gel electrolytes have exhibited storage

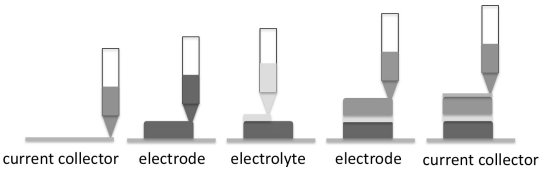


FIGURE 3. SCHEMATIC OF DISPENSER PRINTING OF MULTILAYER ELECTROCHEMICAL ENERGY STORAGE DEVICES.

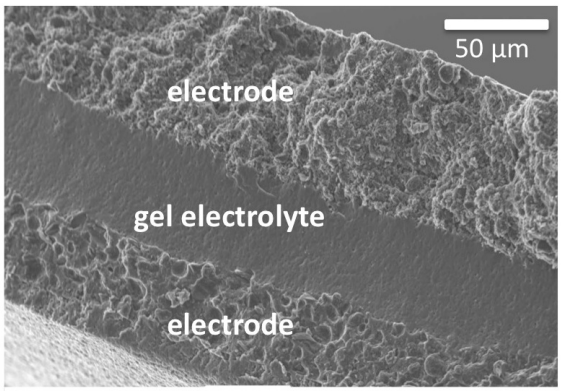


FIGURE 4. CROSS SECTION OF PRINTED ELECTROCHEMICAL CAPACITOR.

capacities as high as 2 mAh/cm$^2$ (Ho et al., 2009). Similarly, carbon supercapacitors using gel electrolytes with 100 mF/cm$^2$ capacitances have been demonstrated with excellent cycle performance (beyond 120,000 cycles without performance degradation) (Ho et al., 2008).

Since all printing steps are performed at room temperature and ambient conditions, the dispenser printer has the added capability of being able to precisely pattern intricate structures directly onto a crowded substrate without damaging any neighboring components. This opens the possibility for integrating various printed structures, such as batteries and capacitors, with other components in a single package. As a demonstration, the physical integration of two elements of a permanent micropower supply is shown in Figure 5. A carbon supercapacitor was printed onto the empty silicon die space surrounding two MEMS fabricated vibration energy harvesting devices (Miller et al., 2009). Furthermore, the versatility of the printer allows for the integration of components onto other substrates such as the outer packaging or backside of a device.

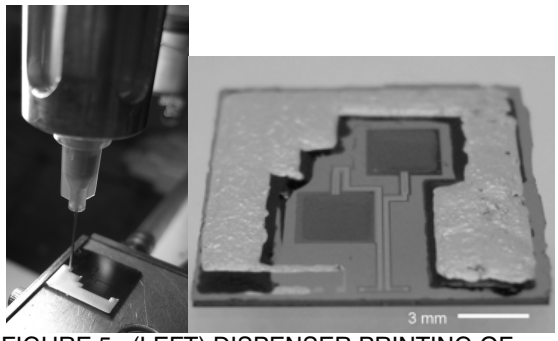


FIGURE 5. (LEFT) DISPENSER PRINTING OF ELECTROCHEMICAL CAPACITOR ON OPEN SPACE SURROUNDING VIBRATIONAL ENERGY HARVESTERS (RIGHT) INTEGRATED MICROPOWER SUPPLY.

## Thermoelectric Energy Harvesters

Thermoelectric micro-devices are attractive thermal energy harvesters because they directly convert thermal gradients into electrical power. They are silent, require no moving parts and have proven reliability through extended use (Rowe, 2005). While the bulk of thermoelectric research is in novel material synthesis (Hochbaum et al., 2008; Poudel et al., 2008), less attention has been paid to device-level manufacturing. Figure 6 shows a typical schematic of a thermoelectric energy generator.

For thermoelectric devices to be practical as energy harvesters from low-grade waste heat sources (1-10 Kelvin gradients), the voltage and power outputs need to be at least 0.5 V and 10 µW, respectively (Chee et al., 2008; Hudak et al., 2008). Since the voltage output of thermoelectric devices scale proportionally with the number of thermoelectric couples, micro-scale thermoelectric devices require high-density thermocouple arrays (typically 1000-2000 couples) within a small device footprint to achieve the voltage requirements (Chen et al., 2009). Previous design studies have shown that

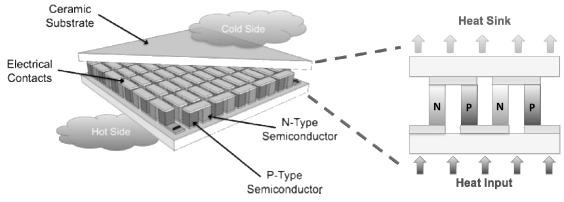


FIGURE 6. SCHEMATIC OF A TYPICAL THERMOELECTRIC ENERGY GENERATOR

optimal power generation occurs when the thermoelectric elements leg lengths are between 100-200 μm for microscale generators (Strasser et al., 2004; Glatz et al., 2006). As the element height decreases, the thermal contact resistances of the hot and cold sinks are no longer negligible, and the effective temperature drop across the active elements becomes small in relation to the total temperature drop of the system. Modeling has shown that optimized geometry designs coupled with standard bismuth telluride-based alloys are capable of producing up to 50 μW/cm$^2$ (Glatz et al., 2006; Chen et al., 2009).

While the necessary power output from micro-scale thermoelectric generators is theoretically feasible, the required device dimensions present a challenge for standard mass production manufacturing techniques. Traditional bulk thermoelectric elements prepared by dicing and extrusion are limited by the resolution of the dicing step to >300 μm thermoelectric leg lengths (Rowe, 2005). Alternatively, conventional microfabrication processes involving lithography and thin-film vapor deposition are limited to < 60 μm element leg lengths (Rowe, 2005; Hudak et al., 2008). There exists a gap in the available technologies for producing optimized thermoelectric devices with 100–200 μm leg lengths. Thus, the prototype dispenser printer provides a viable and scalable fabrication method for additively creating microscale thermoelectric generators.

The dispenser printer is used to print thermoelectric inks containing suspensions of active thermoelectric materials in polymer binders. The active thermoelectric material used is bismuth telluride powder processed using high-energy ball-milling techniques, while the polymer binder consists of an epoxy resin. The thermoelectric inks are then filled and cured in prefabricated polydimethylsiloxane (PDMS) mold templates to create thermoelectric elements. Initial materials have shown promising thermoelectric behavior, and work is currently being performed to improve the properties of the materials (Chen et al., 2009).

Figure 7 shows the fabrication steps for a dispenser-printed thermoelectric device. The fabrication steps are detailed as follows. (1) The dispenser printer first additively deposits the bottom interconnects on a substrate using a conductive silver paste. (2) The PDMS mold with

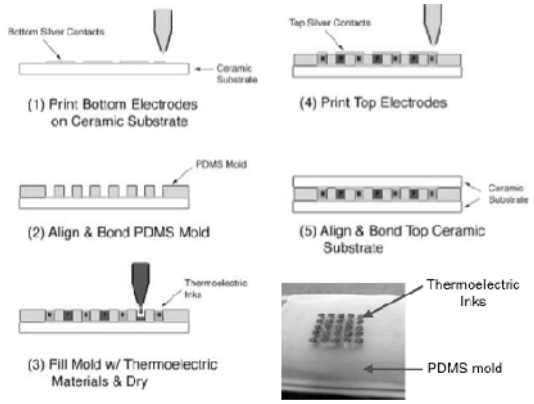


FIGURE 7. FABRICATION STEPS AND IMAGE OF DISPENSER-PRINTED THERMOELECTRIC MODULES

the required geometry design is aligned and bonded to the substrate using an oxygen-plasma bonding process (Tegal Plasmod). (3) Next, holes in the mold are selectively filled with thermoelectric materials using the dispenser printer and cured at 200°C to form the active elements. (4) The top silver interconnects are then printed to link the active elements. (5) Finally, the top substrate is bonded to the mold using the same method as step 2 to complete the device. The PDMS molds with optimal device geometries are fabricated using a double-casting process from an aluminum mold with the final design. Figure 7 also shows a PDMS mold filled with thermoelectric inks. Initial prototypes have 1 mm diameter holes and 1.5 mm leg lengths. Holes as small as 500 μm have been fabricated while smaller holes for higher couple densities are possible. With a goal of filling 100–200 μm holes, the 5 μm repeatability and 1 μm resolution of the printer is capable of fabricating devices with enough precision. Further work is currently being performed to overcome post-processing difficulties involved in completing devices (Chen et al., 2009).

## CONCLUSION

Dispenser printing is a versatile and scalable technique for depositing and patterning functional materials on a variety of substrates. We have analyzed and demonstrated a prototyping dispenser printer capable of fabricating electrochemical energy devices and thermoelectric energy harvesters. Initial work has shown the printing to be a viable and precise technique, particularly for thick-film

applications. Further work is being performed to improve misalignment errors for smaller scale applications. Besides the microscale devices presented in this work, this versatile dispenser printing system has also been applied to other applications such as the precise deposition of magnetic materials on the ends of MEMS cantilever sensors (Leland et al., 2009) and the resonance tuning of vibration energy harvesters (Miller et al., 2009).

## ACKNOWLEDGMENTS

The authors thank the California Energy Commission for supporting this research under contract 500-01-43. We would also like to thank Dan Steingart, Mike Koplow, Andrew Pullin, Christopher Sherman, Ryan Xie, Peter Minor, Ba Quan, Deepa Madan, Brian Mahlstedt, Lindsay Miller, Eli Leland and all our colleagues in the Berkeley Manufacturing Institute for their contributions.

## REFERENCES

Chee, Y., M. Koplow, M. Mark, N. Pletcher, M. Seeman, F. Burghardt, D. Steingart, J. Rabaey, P. Wright, S. Sanders (2008). "PicoCube: A 1 $cm^3$ sensor node powered by harvested energy." *Proceedings of 45th Annual Design Automation Conference,* pp. 114-119.

Chen A., M. Koplow, D. Madan, P.K. Wright, J.W. Evans (2009). "Dispenser printed microscale thermoelectric generators for powering wireless sensor networks." ASME International Mechanical Engineering Congress & Exposition (Lake Buena Vista, 13-19 Nov. 2009), to be published.

Dudney, N.J. (2005). "Solid-state thin film rechargeable batteries." *Materials Science and Engineering B*, Vol. 116, pp. 245-249.

Glatz, W., S. Muntwyler, and C. Hierold (2006). "Optimization and fabrication of thick flexible polymer based micro thermoelectric generator." *Sensors and Actuators A: Physical*, Vol. 132, pp. 337-345.

Ho, C.C., J.W. Evans, and P.K. Wright (2009). "Direct write dispenser printing of zinc microbatteries." *Proceedings of 9th PowerMEMS Workshop,* to be published.

Ho, C.C., D.A. Steingart, J.W. Evans, and P.K. Wright (2008). "Tailoring electrochemical capacitor energy storage using direct write dispenser printing." *ECS Transactions,* Vol. 16 (1), pp. 35-47.

Hochbaum, A.I., R. Chen, R.D. Delgado, W. Liang, E.C. Garnett, M. Najarian, A. Majumdar, and P. Yang (2008). "Enhanced thermoelectric performance of rough silicon nanowires." *Nature,* Vol. 451, pp. 163-167.

Hon, K.K.B., L. Li, and I.M. Hutchings (2008). "Direct writing technology - Advances and developments." *Annals of the CIRP – Manufacturing Technology*, Vol. 57, pp. 601-620.

Hudak, N.S. and G.G. Amatucci (2008). "Small-scale energy harvesting through thermoelectric, vibration, and radiofrequency power conversion." *Journal of Applied Physics*, Vol. 103, pp. 101301.

Leland, E.S, P.K. Wright, and R.W. White (2009). "A MEMS AC current sensor for residential and commercial electricity end-use monitoring." *Journal of Micromechanics and Microengineering,* Vol. 19, pp. 094018.

Lewis, J.A. and G.M. Gratson (2004). "Direct writing in three dimensions." *Materials Today*, Vol. 7, pp. 32-39.

Lim, J., D. Choi, H. Kim, W. Cho, and Y. Yoon (2001). "Thin film supercapacitors using a sputtered $RuO_2$ electrode." *Journal of The Electrochemical Society*, Vol. 148 (3), pp. A275-A278.

Miller, L.M., C.C. Ho, P.C. Shafer, P.K. Wright, J.W. Evans, and R. Ramesh (2009). "Integration of a low frequency, tunable MEMS piezoelectric energy harvester and a thick film micro capacitor as a power supply system for wireless sensor nodes." *Proceedings of IEEE Energy Conversion Congress and Exposition,* pp. 2627-2634.

Poudel, B., Q. Hao, Y. Ma, Y. Lan, A. Minnich, B. Yu, X. Yan, D. Wang, A. Muto, D. Vashaee, X, Chen, J. Liu, M.S. Dresselhaus, G. Chen, and Z. Ren (2008). "High-thermoelectric performance of nanostructured bismuth antimony telluride bulk alloys." *Science,* Vol. 320, pp. 634-638.

Rowe, D.M. (2005). *Thermoelectrics Handbook: Macro to Nano.* Boca Raton, FL: Taylor and Francis Group, LLC.

Strasser, M., R. Aigner, C. Lauterbach, T.F. Sturm, M. Franosch, and G. Wachutka (2004). "Micromachined CMOS thermoelectric generators as on-chip power supply." *Sensors & Actuators A,* Vol. 114, pp. 362-370.